

# Cyclotron enhancement of tunneling

M. V. Medvedeva,<sup>1</sup> I. A. Larkin,<sup>2,3</sup> S. Ujevic,<sup>2</sup> L. N. Shchur,<sup>1</sup> and B. I. Ivlev,<sup>4,5</sup>

<sup>1</sup>*Landau Institute for Theoretical Physics, Moscow, Russia,*

<sup>2</sup>*International Center of Condensed Matter Physics, Brasilia, Brazil*

<sup>3</sup>*Institute of Microelectronics Technology, Chernogolovka, Russia*

<sup>4</sup>*Universidad Autónoma de San Luis Potosí, San Luis Potosí, Mexico,*

<sup>5</sup>*Department of Physics and Astronomy and NanoCenter,  
University of South Carolina, Columbia, South Carolina, USA*

A state of an electron in a quantum wire or a thin film becomes metastable, when a static electric field is applied perpendicular to the wire direction or the film surface. The state decays via tunneling through the created potential barrier. An additionally applied magnetic field, perpendicular to the electric field, can increase the tunneling decay rate for many orders of magnitude. This happens, when the state in the wire or the film has a velocity perpendicular to the magnetic field. According to the cyclotron effect, the velocity rotates under the barrier and becomes more aligned with the direction of tunneling. This mechanism can be called cyclotron enhancement of tunneling.

PACS numbers: 03.65.Xp, 03.65.Sq

## I. INTRODUCTION

Tunneling in a magnetic field is a matter of investigation for many years. The magnetic field can influence tunneling across a potential barrier in two different ways.

First, the magnetic field can modify an underbarrier motion related to a classically forbidden region. Studies of this phenomenon are presented in the literature. In Refs. [1, 2] it was pointed out that an underbarrier fall of the wave function can be less rapid in an inhomogeneous sample. See also Refs. [3, 4, 5, 6, 7]. In Ref. [8] a transmission coefficient through a quadratic barrier was found. A decay of a metastable state was considered in Ref. [9]. The certain peculiarities of an underbarrier wave function were discussed in Refs. [10, 11].

Second, the magnetic field can influence a state of an electron at a classically allowed region after an exits from under the barrier. A typical example is the Wigner resonance when the electron tunnels into a potential well with a level aligned to its energy [12]. See experimental measurements, for instance, in Refs. [13, 14, 15]. Another example relates to a specific density of states in the classical region after the tunneling barrier. A state of an electron, influenced by the magnetic field, may fit better that density of states and this results in increase of tunneling rate [16].

The goal of the paper is to study tunneling decay rate of a metastable state in a magnetic field (the electron after tunneling goes to infinity). The question to be answered: Can a magnetic field increase the decay rate? It is clear that the above effect of density of states at the region after the barrier can, in principle, increase the rate. But this effect, related to a prefactor, cannot be very large. According to Ref. [16], there is approximately 50% enhancement of the effect.

It would be much more amazing to increase the main exponential part of the decay rate by the magnetic field. The references [1, 2, 3, 4, 5, 6, 7, 8, 9] say that it is impossible. Indeed, when an electron enters under the barrier

its velocity deviates, due to the cyclotron effect, from a tunneling path with no magnetic field. This leads to a reduction of the tunneling probability by the magnetic field. The reduction can be also explained in terms of increasing of the total barrier. The additional barrier is proportional to a squared velocity of the electron in the magnetic field [1, 2].

But there is a situation when the electron tunnels from a quantum wire or another object extended in the direction perpendicular to tunneling. In this case a state prior to tunneling can have a finite velocity perpendicular to the tunneling direction. According to the cyclotron effect, this velocity rotates under the barrier and becomes more aligned with the tunneling direction. This leads to enhancement of the tunneling rate by the magnetic field (cyclotron enhancement).

Formally, cyclotron enhancement of tunneling results from a reduction of the main tunneling exponent which reminds one of Wentzel, Kramers, and Brillouin (WKB). The exponent can be reduced in a few times. Suppose that at zero magnetic field the tunneling rate is proportional to  $10^{-24}$ . The magnetic field can turn it into, say,  $10^{-7}$ .

We consider in the paper tunneling from a straight quantum wire, directed in the  $y$  axis, embedded into a two-dimensional electron system in the  $\{x, y\}$  plane. The potential barrier is created by the electric field  $\mathcal{E}_0$  directed along the  $x$  axis (the direction of tunneling). The magnetic field  $H$  is aligned along  $z$ . According to electrodynamics, after tunneling a motion of the electron in perpendicular magnetic and electric fields is restricted by a finite interval in the  $x$  direction [17]. To get the electron passed to the infinite  $x$  one should put some potential wall(s) along the  $x$  direction restricting the  $y$  motion. Due to multiple reflections from the restricting wall in the magnetic field the electron goes to the infinite  $x$ . We model the walls by the potential proportional to  $y^4$ .

The theory presented relates also to tunneling from a

flat  $\{y, z\}$  film with quantized electron motion in the  $x$  direction. The electron tunnels into a three-dimensional reservoir. Restricting walls should be placed parallel to the  $\{x, z\}$  plane.

Without the restricting walls a solution can be obtained analytically on the bases of the modified WKB approach as shown in Sec. III. An approximation of classical complex trajectories is formulated in Sec. IV. In Secs. V and VI two different methods of numerical calculations are applied to the problem with restricting walls.

## II. FORMULATION OF THE PROBLEM

We consider an electron localized in the  $\{x, y\}$  plane. The static magnetic field  $H$  is directed along the  $z$  axis. Suppose a motion of the electron in the  $\{x, y\}$  plane to occur in the potential  $U(x, y)$ . Then the Schrödinger equation, with the vector potential  $\vec{A} = \{0, Hx, 0\}$ , has the form [12]

$$-\frac{\hbar^2}{2m} \frac{\partial^2 \psi}{\partial x^2} - \frac{\hbar^2}{2m} \left( \frac{\partial}{\partial y} + ix \frac{m\omega_c}{\hbar} \right)^2 \psi + U(x, y)\psi = E\psi, \quad (1)$$

where  $\omega_c = |e|H/mc$  is the cyclotron frequency. The potential

$$U(x, y) = -\hbar \sqrt{\frac{2u_0}{m}} \delta(x) - \mathcal{E}_0 x + u_0 \frac{y^4}{a^4} \quad (2)$$

describes the quantum wire placed in the  $y$  direction (the first term), the constant electric field  $\mathcal{E}_0$  (the second term), and the restricting walls in the  $y$  direction are modeled by the third term. At  $\mathcal{E}_0 = 0$  and  $H = 0$  the discrete energy level in the  $\delta$  well ( $-u_0$ ) is a ground state in the WKB approximation.

### A. Dimensionless units

Let us introduce the dimensionless electric field  $\varepsilon$  and the magnetic field  $h$  by the equations

$$\varepsilon = \frac{a\mathcal{E}_0}{u_0}, \quad h = \frac{\omega_c}{\mathcal{E}_0} \sqrt{\frac{mu_0}{2}}. \quad (3)$$

Below we measure  $x$  and  $y$  in the units of  $u_0/\mathcal{E}_0$  and time in the units of

$$\tau_{00} = \frac{\sqrt{2mu_0}}{\mathcal{E}_0}. \quad (4)$$

The energy is  $E = u_0\lambda$  where the dimensionless energy  $\lambda$  is negative in our problem. We also introduce a large semiclassical parameter

$$B = \frac{u_0 \sqrt{2mu_0}}{\hbar \mathcal{E}_0}. \quad (5)$$

At zero magnetic field ( $h = 0$ ) the WKB probability of tunneling [12]

$$w(h = 0) \sim \exp\left(-\frac{4B}{3}\right) \quad (6)$$

is small. In the new variables Schrödinger equation (1) has the form

$$-\frac{1}{B^2} \frac{\partial^2 \psi}{\partial x^2} - \left( \frac{1}{B} \frac{\partial}{\partial y} + ihx \right)^2 \psi + \left[ \frac{y^4}{\varepsilon^4} - x - \frac{2}{B} \delta(x) \right] \psi = \lambda \psi. \quad (7)$$

One can exclude the point  $x = 0$ , if to impose the boundary condition

$$\frac{\partial \psi}{\partial x} \Big|_{x=+0} - \frac{\partial \psi}{\partial x} \Big|_{x=-0} = -2B\psi(0, y). \quad (8)$$

With the semiclassical accuracy, the lowest level at the  $\delta$  well is  $\lambda = -1$ . At a finite electric field that level is metastable and we should find a decay rate due to tunneling in the magnetic field.

### B. A semiclassical approach

When the potential barrier is hardly transparent (a large  $B$ ) one can use the semiclassical approximation for the wave function [12]

$$\psi(x, y) \sim \exp[iB\sigma(x, y)], \quad (9)$$

where  $\sigma(x, y)$  is the classical action satisfying the equation of Hamilton-Jacobi at  $x \neq 0$

$$\left( \frac{\partial \sigma}{\partial x} \right)^2 + \left( \frac{\partial \sigma}{\partial y} + hx \right)^2 - x + \frac{y^4}{\varepsilon^4} = \lambda. \quad (10)$$

The function  $\sigma(x, y)$  is continuous. As follows from Eq. (10),  $(\partial\sigma/\partial x)^2$  is also continuous. According to that, one can consider the action at positive  $x$  with the boundary condition

$$\frac{\partial \sigma}{\partial x} \Big|_{x=0} = i, \quad (11)$$

which follows from Eq. (8). In the approximation of a large  $B$  the condition (8) is reduced to

$$\frac{\partial \psi(x, y)}{\partial x} \Big|_{x=0} = -B\psi(0, y), \quad (12)$$

if to consider the problem at positive  $x$  only.

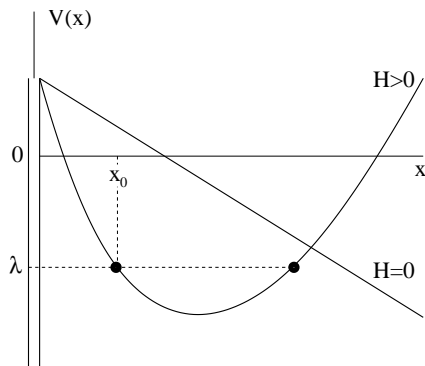


FIG. 1: The effective potential energy (15) is plotted for a positive  $k$  in Eq. (16). An electron tunnels between  $x = 0$  and  $x_0$ . The two dots mark terminal points between which a classical motion occurs. The potential barrier with no magnetic field is shown by the straight line.

### III. CYCLOTRON ENHANCEMENT OF TUNNELING

First, we consider tunneling from the quantum wire, when there are no restriction of the motion in the  $y$  direction. In other words, we drop down the term  $y^4$  in the potential  $U(x, y)$  (2). In this case the solution of the Schrödinger equation (1)

$$\psi(x, y) = \exp(-iBky) \varphi(x) \quad (13)$$

is determined by the effective Schrödinger equation

$$-\frac{1}{B^2} \frac{d^2 \varphi}{dx^2} + V(x) \varphi = \lambda \varphi \quad (14)$$

with the effective potential energy

$$V(x) = (k - hx)^2 - x - \frac{2}{B} \delta(x). \quad (15)$$

The first term in Eq. (15) is proportional to squared velocity of the electron. Solutions with positive and negative wave vector  $k$  are possible according to different directions of motion in the wire. In the WKB approximation for the state, localized in the  $\delta$  well,

$$k = \pm \sqrt{1 + \lambda}. \quad (16)$$

In the physical units, the velocity along the quantum wire is

$$v_y = \mp \sqrt{1 + \lambda} \sqrt{\frac{2u_0}{m}}. \quad (17)$$

Below we consider a positive  $k$  related to the motion from  $+\infty$  to  $-\infty$  in  $y$ . For this case the potential energy  $V(x)$  is shown schematically in Fig. 1 and the WKB wave function under the barrier,  $0 < x < x_0$ , has the form

$$\psi(x, y) \sim \exp(-iyB\sqrt{1 + \lambda}) \exp \left[ -B \int_0^x dx_1 \sqrt{(\sqrt{1 + \lambda} - hx_1)^2 - x_1 - \lambda} \right]. \quad (18)$$

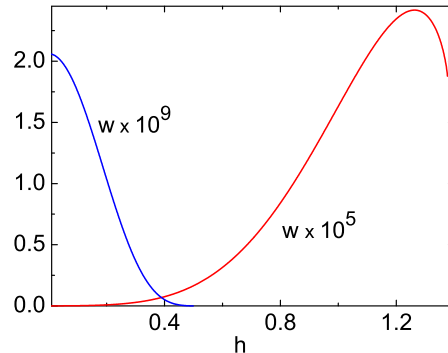


FIG. 2: (Color online) The decay rate (22) of the metastable state of the quantum wire versus magnetic field  $h$  at  $B = 15$ . Left curve: The state in the wire has zero velocity parallel to the wire,  $\lambda = -1$ . Right curve: The same when the velocity is finite,  $\lambda = -0.594$ .

The classical terminal point, determined by the condition  $V(x) = \lambda$ , is

$$x_0 = \frac{1}{h} \left( \sqrt{1 + p^2} - p \right), \quad (19)$$

where

$$p = \sqrt{\left( \frac{1}{2h} + \sqrt{1 + \lambda} \right)^2 - 1}. \quad (20)$$

The terminal point  $x_0$  plays a role of the exit point from under the barrier and is marked in Fig. 1. The classically allowed region,  $V(x) < \lambda$ , is between two terminal points displayed in Fig. 1. Our consideration has a meaning, when the classically allowed region is of a finite width. This occurs under the condition

$$h < \frac{1}{2(1 - \sqrt{1 + \lambda})}, \quad (21)$$

when the two terminal points in Fig. 1 are separated.

For the  $y$ -independent potential considered the classically allowed motion occurs between the two terminal points in Fig. 1. It means that after an exit from under the barrier the electron motion will remain restricted in the  $x$  direction. A penetration through the barrier,  $0 < x < x_0$ , in Fig. 1 can be enhanced, when the level  $\lambda$  in the  $\delta$  well coincides with one of the discrete levels in the well at  $x > x_0$ . The Wigner resonant tunneling occurs in this case [12].

A scenario becomes different, if we return to the full potential energy (2). After coming from under the barrier the electron participates in cyclotron motion and the Lorentz drift similar to a classical particle. The Lorentz drift in the potential  $(u_0 y^4 / a^4 - \mathcal{E}_0 x)$  brings the electron to the infinite  $x$ . This happens, according to electrodynamics, as a result of multiple reflections from the “wall”

$u_0 y^4/a^4$  [17]. In that case Wigner tunneling does not occur since there are no discrete levels to the right of the barrier. This situation corresponds to a decay of the metastable state in the  $\delta$  well since after tunneling the electron goes to the infinite  $x$ .

Whereas the potential  $y^4$  strongly disturbs the motion at the classical region, the underbarrier motion along the direction  $y = 0$  is hardly violated since reflections from that potential under the barrier are less important. It is shown in Sec. V. For this reason, for an underbarrier motion in the full potential (2) one can use the approach, when the potential  $y^4$  is dropped down. Accordingly, in the semiclassical approximation the tunneling rate is given by the WKB formula

$$w \sim \exp \left[ -\frac{B}{h} \left( \sqrt{1+p^2} - p^2 \ln \frac{1+\sqrt{1+p^2}}{p} \right) \right], \quad (22)$$

which follows from Eq. (18) as  $|\psi(x_0, y)|^2$ .

For zero magnetic field,  $h = 0$ , the tunneling rate (22) does not depend on  $\lambda$  and coincides with the conventional WKB expression (6). For  $B = 15$  and  $\lambda = -1$  the tunneling rate in Fig. 2 drops down with the magnetic field, as usually, since the metastable state in the quantum wire has zero momentum (16) perpendicular to tunneling. For  $B = 15$  and  $\lambda > -1$  such a momentum is finite resulting in cyclotron enhancement of tunneling. In Fig. 2 we plot the tunneling rate for  $\lambda = -0.594$ . This value is chosen to have a link to numerical data discussed below.

#### IV. CLASSICAL TRAJECTORIES

For the potential (2) analytical solutions of the Schrödinger equation (7) and the Hamilton-Jacobi equation (10) do not exist. Nevertheless, to calculate a tunneling rate with the exponential accuracy it is not necessary to solve the Hamilton-Jacobi equation (10) in the full  $\{x, y\}$  plane. It is sufficient to track  $\sigma(x, y)$  along a classical trajectory  $\{x(\tau), y(\tau)\}$ , where  $\tau = -it$  is imaginary time since an underbarrier classical motion is impossible.

The method of classical trajectories in imaginary time is well developed for static potential barrier with no magnetic field [18, 19, 20, 21]. In this case the main contribution to a tunneling rate comes from the extreme path linking two classically allowed regions. The real underbarrier path  $\{x(\tau), y(\tau)\}$  can be parametrized as a classical trajectory in imaginary time.

A situation with a magnetic field is substantially different. For the potential (2) in a magnetic field the coordinate  $x(\tau)$  remains real in the underbarrier motion but  $y(\tau) = -i\eta(\tau)$  becomes imaginary. This means that the trajectory does not track the entire underbarrier path as for zero magnetic field. It just provides a ‘‘bypass’’ through the plane of complex  $y$ . So the method of classical trajectories for tunneling in a magnetic field is non-trivial.

One should note that the same situation takes place for tunneling across nonstationary barriers where imaginary time stands instead of imaginary  $y$ . Validity of the non-trivial trajectory method for the nonstationary barrier was numerically proved in Ref. [22]. The numerical results of the present paper support the trajectory method also for a static magnetic field.

We consider tunneling from the  $\delta$  well ( $\tau = \tau_0$ ) to the classically allowed region ( $\tau = 0$ ). The ratio of the densities

$$w = \frac{|\psi(x(0), 0)|^2}{|\psi(0, 0)|^2} \quad (23)$$

can be identified with a tunneling rate. With the semiclassical accuracy,  $w \sim w_T$ , where

$$w_T = \exp(-2B \text{Im}[\sigma(x(0), 0) - \sigma(0, 0)]) \quad (24)$$

is the tunneling exponent. The trajectory method allows to calculate the part

$$A_0 = 2B \text{Im}[\sigma(x(0), 0) - \sigma(0, -i\eta(i\tau_0))] \quad (25)$$

of the total action (24) only. This part is expressed through the classical trajectory

$$A_0 = 2B \int_0^{\tau_0} d\tau \left[ \frac{1}{4} \left( \frac{\partial x}{\partial \tau} \right)^2 - \frac{1}{4} \left( \frac{\partial \eta}{\partial \tau} \right)^2 - hx \frac{\partial \eta}{\partial \tau} - x + \frac{\eta^4}{\varepsilon^4} - \lambda \right]. \quad (26)$$

See, for example, [10, 11]. The expression in the square brackets is the Lagrangian in terms of imaginary time. The coordinates  $x(\tau)$  and  $\eta(\tau)$  in Eq. (26) are solutions of the classical equations of motion

$$\frac{1}{2} \frac{\partial^2 x}{\partial \tau^2} = -h \frac{\partial \eta}{\partial \tau} - 1, \quad \frac{1}{2} \frac{\partial^2 \eta}{\partial \tau^2} = -h \frac{\partial x}{\partial \tau} - \frac{4\eta^3}{\varepsilon^4} \quad (27)$$

with the conditions

$$x(\tau_0) = 0, \quad \left. \frac{\partial x}{\partial \tau} \right|_{\tau_0} = -2, \quad \eta(0) = 0, \quad \left. \frac{\partial \eta}{\partial \tau} \right|_0 = 0. \quad (28)$$

Since the trajectory terminates at the  $\delta$  well, this leads to the first condition (28). The second condition (28) results from Eq. (11). The third condition (28) corresponds to the physical exit point  $y = 0$ . The fourth condition (28) is a property of an exit point where the electrons stops to move in the tunneling direction. Note, that the physical velocity perpendicular to the tunneling direction at the exit point from under the barrier is not zero. In the dimensionless units used it is

$$\frac{\partial y}{\partial t} = -\left. \frac{\partial \eta}{\partial \tau} \right|_{\tau_0}. \quad (29)$$

A solution of Eqs. (27) corresponds to the total energy

$$\lambda = -\frac{1}{4} \left( \frac{\partial x}{\partial \tau} \right)^2 + \frac{1}{4} \left( \frac{\partial \eta}{\partial \tau} \right)^2 - x + \frac{\eta^4}{\varepsilon^4}. \quad (30)$$

The relation (30) is the fifth condition to the equations (27) which can be satisfied by a proper choice of  $\tau_0$ .

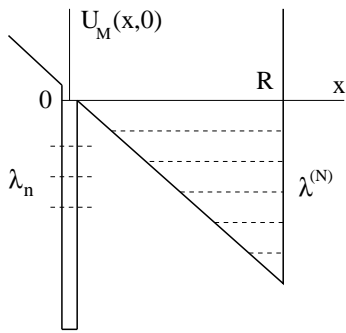


FIG. 3: The modified potential with the infinite wall at  $x = R$ . The discrete energy levels  $\lambda_n$  are associated with the  $\delta$  well. The levels  $\lambda^{(N)}$  are connected with the triangular well.

### A. Total action

The trajectory terminates at the unphysical (complex) point  $x = 0$ ,  $y = -i\eta(\tau_0)$ . One should connect this point with a physical one, for example,  $x = 0$ ,  $y = 0$ . In other words, one should add to  $A_0$  the action

$$A_1 = 2B\text{Im}[\sigma(0, -i\eta(i\tau_0)) - \sigma(0, 0)]. \quad (31)$$

to complete the tunneling exponent (24). One can find the action (31) by a direct solution of the Hamilton-Jacobi equation (10). Since the condition (11) holds at all  $y$ , it follows from (10) that

$$\left(\frac{\partial\sigma(0, y)}{\partial y}\right)^2 + \frac{y^4}{\varepsilon^4} = 1 + \lambda. \quad (32)$$

The integration results in

$$A_1 = 2B\varepsilon(1 + \lambda)^{3/4} f\left[\frac{\eta(\tau_0)}{\varepsilon(1 + \lambda)^{1/4}}\right] \text{sgn}\left(\frac{\partial\eta}{\partial\tau}\bigg|_{\tau_0}\right), \quad (33)$$

where

$$f(z) = \int_0^z dv \sqrt{1 - v^4}. \quad (34)$$

The sign term in Eq. (33) accounts for a correct sign of the square root just to match the solution at the point  $x = 0$ ,  $y = -i\eta(\tau_0)$ . So the tunneling rate is given by

$$w \sim \exp(-A_0 - A_1), \quad (35)$$

where the parts of the total action are determined by Eqs. (26) and (33).

It is not difficult to check that, if to formally drop down the part  $y^4$  in the potential (2), the trajectory formalism (35) gives the same result (22). For this purpose one has to write down the explicit expression for the classical trajectory

$$\eta(\tau) = \frac{\sinh(2h\tau)}{h \sinh(2h\tau_0)} - \frac{\tau}{h}, \quad (36)$$

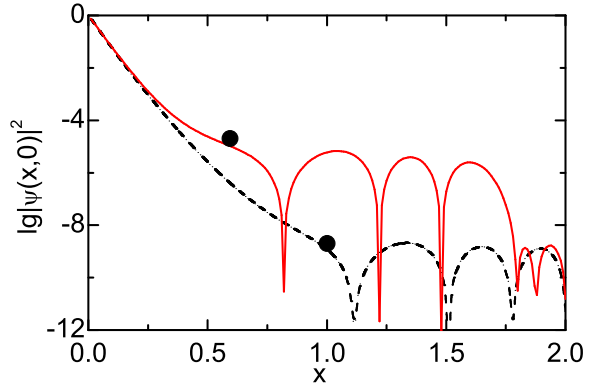


FIG. 4: (Color online) Decimal logarithm of the electron density at  $B = 15$  calculated by the method of Sec. V. The dashed curve: Zero magnetic field,  $h = 0$ . The solid curve: The finite magnetic field,  $h = 1.1$ , and the eigenvalue at the wire  $\lambda_n = -0.594$ . The two dots mark the classical exit points calculated from Eqs. (18) and (19).

which follows from Eqs. (27), if to drop down the nonlinear part in  $\eta$ . The total underbarrier time is determined by the relation

$$p \sinh(2h\tau_0) = 1. \quad (37)$$

One should also put  $f(z) = z$  in Eq. (33). At the terminal time  $\tau_0$ , as follows from Eqs. (36) and (37),

$$\eta(\tau_0) = \frac{1}{h} - \frac{1}{2h^2} \ln \frac{1 + \sqrt{1 + p^2}}{p}. \quad (38)$$

### V. NUMERICAL CALCULATIONS BY THE X - Y NET

For numerical studies of the problem we consider the Schrödinger equation (7) at positive  $x$  with the boundary condition (12). Since in numerical calculations an infinite  $x$  is impossible we modify the potential  $U(x, y)$  (2) adding the infinite potential wall at  $x = R$ . The wall is accounted for by the condition  $\psi(R, y) = 0$ . In Fig. 3 the modified potential  $U_M(x, 0)$  is shown, where the electron is completely localized resulting in discrete eigenvalues of energy  $\lambda$ . In the  $\delta$  well, due to the potential  $y^4/\varepsilon^4$ , there are discrete levels  $\lambda_n$ . With no  $y^4$  potential the set  $\lambda_n$  becomes continuous. The levels associated with the triangular well are  $\lambda^{(N)}$ .

For the potential  $U(x, y)$  (2) an electron, initially localized at the  $\delta$  well, can go to the infinite  $x$  providing a decay of this metastable state during the typical time  $t_0 \sim 1/w_T$ , where  $w_T$  is the tunneling exponent (24).

For a state, initially localized at the  $\delta$  well of the potential  $U_M(x, y)$ , the same type of time  $t_0 \sim 1/w_T$  is

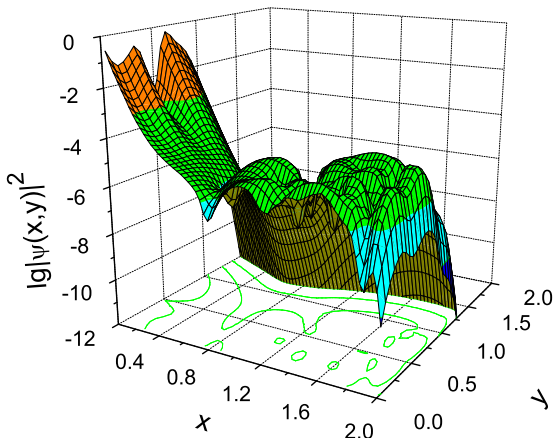


FIG. 5: (Color online) The three-dimensional plot of the decimal logarithm of the electron density for  $h = 1.1$ ,  $\lambda = -0.594$ , and  $B = 15$ .

required to spread out to the triangular well when  $\lambda_n$  is not equal to  $\lambda^{(N)}$ , that is we are away from Wigner resonances. The ratio of steady wave functions at the triangular well and at the  $\delta$  well is exponentially small. If to avoid Wigner resonances, it is determined by the same exponent as the tunneling decay rate for the case of an infinite  $R$ . This justifies the use of  $U_M(x, y)$ .

When an energy level, occupied by the electron at the  $\delta$  well, coincides with one at the triangular well the Wigner resonant tunneling occurs. In this situation the ratio (23) of steady wave functions at the triangular well and at the  $\delta$  well is not exponentially small. Nevertheless, the time to fill out the initially empty triangular well still remains exponentially long,  $t_0 \sim 1/\sqrt{w_T}$ .

We numerically calculated  $\psi(x, y)$  for the potential  $U_M(x, y)$  using the discrete two-dimensional net in  $\{x, y\}$  space. A step was chosen from a condition of a better convergence. The method used works well for hyperbolic system and does not result in unphysical exponents. We started with the asymptotic  $\psi \sim \exp(-By^3/3\varepsilon)$  at  $y \rightarrow \infty$  and chosen eigenvalues of  $\lambda$  from the condition of  $\partial|\psi|/\partial y = 0$  at  $y = 0$ . In the calculations we put  $B = 15$ ,  $\varepsilon = 1$ , and  $R = 2$ . The calculations are performed at the interval  $0 < x < 2$  with the boundary condition (12) at  $x = 0$ . A distance between energy levels in Fig. 3 can be estimated from the semiclassical approach [12] as  $(\lambda_{n+1} - \lambda_n) \sim (\lambda^{(N+1)} - \lambda^{(N)}) \sim 0.1 - 0.2$ . This is confirmed by the numerical calculations.

The results are figured out in Fig. 4.

At zero magnetic field,  $h = 0$ , the variables are separated and  $\psi(x, 0)$  is a solution of the effective Schrödinger equation (14) with the potential (15), where one has to add the wall at  $x = 2$  and formally put  $k = h = 0$  and  $\lambda \simeq -1$ . The wave function is shown in Fig. 4 by the

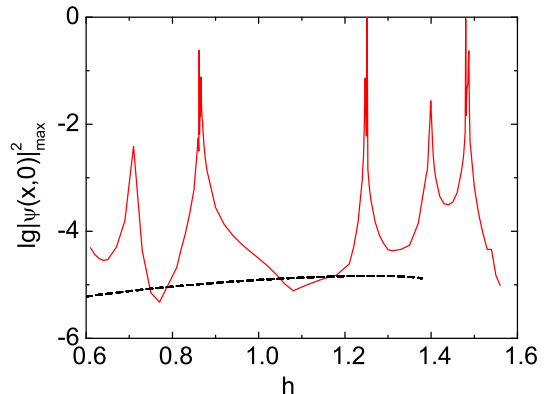


FIG. 6: (Color online) Decimal logarithm of the maximal value of the wave function after an exit from under the barrier versus magnetic field  $h$ . The maxima relate to Wigner resonances,  $\lambda_n = \lambda^{(N)}$ . A level in the wire from the interval  $0.55 < \lambda_n < 0.6$  is adjusted to the variable  $h$ . The dashed curve is  $\lg w$  from Fig. 2 with  $\lambda = -0.594$  for comparison. It corresponds to the electron density after the barrier when  $R = \infty$  (no Wigner resonances).

dashed curve. Due to reflections from the wall at  $x = 2$  the wave function oscillates at the interval  $1 < x < 2$ . At the classical exit point  $x = 1$  the wave function, calculated by Eq. (18), is marked by the dot on the dashed curve in Fig. 4 where  $|\psi(1, 0)|^2 \simeq 2 \times 10^{-9}$ .

At the finite magnetic field,  $h = 1.1$ , the numerically calculated wave function is plotted by the solid curve in Fig. 4. The chosen eigenvalue  $\lambda = -0.594$  is one of the discrete levels  $\lambda_n$  in Fig. 3. The wave function is extended over the whole interval  $0 < x < 2$  due to reflections from the potential  $y^4$  and the wall at  $x = 2$  in the magnetic field. A classical exit point  $\{x(0), 0\}$  and  $\psi(x(0), 0)$  can be calculated on the basis of the trajectory method of Sec. IV. The results hardly differ from the case of Sec. III when the potential  $y^4$  was dropped down. According to Eq. (38),  $\eta(\tau_0) \simeq 0.263$  which leads to the very small potential  $y^4 \simeq 0.005$ . It is obvious and also can be shown that an influence of this potential on the classical trajectory is small. We emphasize that in our case the potential  $y^4$  hardly influences the underbarrier motion only. After an exit from under the barrier the electron is strongly reflected by that potential.

Neglecting the part  $y^4$ , one can easily perform trajectory calculations. This results in the exit point (19),  $x_0 = x(0) \simeq 0.594$ , and the electron density  $|\psi(x_0, 0)|^2 \simeq 2.0 \times 10^{-5}$  marked as the dot on the solid curve in Fig. 4. We see that the analytical and numerical results are close to each other for both zero and the finite magnetic fields.

The three-dimensional plot of  $|\psi(x, y)|^2$  is shown in Fig. 5. Due to reflections from the potential  $y^4$  and the wall at  $x = 2$ , the motion covers the whole region apart the barrier. We also performed numerical calculations

for the potential  $y^{16}$  instead of  $y^4$  just to be closer to a situation of an infinite restricting wall. Qualitatively, the wave function looks the same filling out the whole  $\{x, y\}$  space to the right of the barrier.

To get tunneling to the triangular well more adequate to tunneling to an infinite region, we should avoid Wigner resonances, as pointed out above. In Fig. 6 the maximal value of  $|\psi(x, 0)|_{max}^2$  after the exit point is plotted versus  $h$ . As one can see, the structure of Wigner resonances is very pronounced. A shape of the wave functions in the triangular well close to Wigner peaks was checked. We found no deviation from eigenfunctions at the triangular well, when the  $\delta$  well at  $x = 0$  was absent. This proves the Wigner nature of the peaks in Fig. 6. We choose  $h = 1.1$  to get away of the Wigner resonances as clear from Fig. 6.

## VI. NUMERICAL CALCULATIONS BY THE MATRIX FORMALISM

In Sec. V we performed the numerical calculations at the interval  $0 < x < 2$  using the boundary condition (12) at  $x = 0$ . In this section we demonstrate the numerical formalism, which does not explore the boundary condition (12). The calculations are performed at the interval  $-2 < x < 2$ , where the potential  $U_M(x, y)$  is symmetrically continued from the region  $0 < x$  for negative  $x$ . The  $\delta$  function is approximated by a narrow well of the width of one computational step. The same method to model a  $\delta$  well was used in Ref. [22]. For positive  $x$  in the semiclassical approach (a large  $B$ ) the results for the symmetric potential chosen and for the potential  $U_M(x, y)$  should be close to each other. This is confirmed by the numerical calculations.

In this section we use a matrix formalism. We start up with the Schrödinger equation

$$-\left(\frac{1}{B}\frac{\partial}{\partial x} - ih y\right)^2 \psi - \frac{1}{B^2}\frac{\partial^2 \psi}{\partial y^2} + \left[\frac{y^4}{\varepsilon^4} - |x| - \frac{2}{B}\delta(x)\right] \psi = \lambda \psi \quad (39)$$

with the conditions  $\psi(\pm 2, y) = 0$ . Eq. (39) differs from the form (7) by the gauge. The wave function can be written as the expansion

$$\psi(x, y) = \sum_{n=0}^{\infty} F_n(x) \varphi_n(y\sqrt{B}), \quad (40)$$

where  $\varphi_n(z)$  is a normalized eigenfunction of a harmonic oscillator,

$$-\frac{\partial^2 \varphi_n}{\partial z^2} + z^2 \varphi_n = (1 + 2n) \varphi_n. \quad (41)$$

One can easily show that the functions  $F_n(x)$  satisfy the

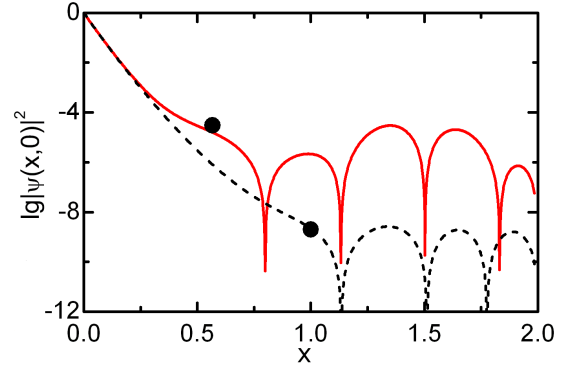


FIG. 7: (Color online) Decimal logarithm of the electron density at  $B = 15$  calculated by the method of Sec. VI. The dashed curve: Zero magnetic field,  $h = 0$ . The solid curve: The finite magnetic field,  $h = 1.1$ , and the eigenvalue of the wire state  $\lambda_n = -0.586$ . The two dots mark the classical exit points  $|\psi(1, 0)|^2 \simeq 2 \times 10^{-9}$  for  $h = 0$  and  $|\psi(0.586, 0)|^2 \simeq 2.3 \times 10^{-5}$  for  $h = 1.1$  calculated from Eqs. (18) and (19).

equations

$$-\frac{1}{B^2}\frac{\partial^2 F_n}{\partial x^2} + \frac{2ih}{B^{3/2}} \sum_{m=0}^{\infty} \beta_n^m \frac{\partial F_m}{\partial x} + \sum_{m=0}^{\infty} \left( \frac{h^2 - 1}{B} \gamma_n^m + \frac{1}{B^2 \varepsilon^4} \alpha_n^m \right) F_m + \left[ \frac{1 + 2n}{B} - |x| - \frac{2}{B} \delta(x) - \lambda \right] F_n = 0, \quad (42)$$

where the matrices  $\alpha_n^m$ ,  $\beta_n^m$ , and  $\gamma_n^m$  are symmetric and

$$\alpha_n^m = \int_{-\infty}^{\infty} dz \varphi_m(z) z^4 \varphi_n(z). \quad (43)$$

The matrix  $\beta_n^m$  ( $\gamma_n^m$ ) is determined by the relation analogous to (43) but with the substitution  $z^4 \rightarrow z$  ( $z^4 \rightarrow z^2$ ). The non-zero elements are

$$\alpha_n^{n-4} = \frac{\sqrt{n(n-1)(n-2)(n-3)}}{4},$$

$$\alpha_n^n = \frac{3(2n^2 + 2n + 1)}{2}, \quad \alpha_n^{n-2} = \frac{(2n-1)\sqrt{n(n-1)}}{2}$$

$$\beta_n^{n-1} = \sqrt{\frac{n}{2}}, \quad \gamma_n^{n-2} = \frac{\sqrt{n(n-1)}}{2}, \quad \gamma_n^n = \frac{1+2n}{2} \quad (44)$$

and also  $\alpha_n^{n+4}$ ,  $\alpha_n^{n+2}$ ,  $\beta_n^{n+1}$ , and  $\gamma_n^{n+2}$  obtained as symmetric combinations from (44) with the shifts of  $n$ .

The above matrix formalism is used to numerically calculate the wave function (40) by a solution of the eigenvalue problem (42). The calculations were performed by means of the discretization of the interval  $-2 < x < 2$



using 513 points. To check the scheme we made additional runs for the interval  $-3 < x < 1$  with the equal number of discrete points. The both methods resulted in the same eigenvalues and eigenfunctions. In all the calculations we considered nine terms in the expansion (40) of the wave function.

The results are displayed in Fig. 7 showing the states generic with ones in Fig. 4. The difference in  $\lambda_n$  for the both figures is 0.008 which is substantially less than  $(\lambda_{n+1} - \lambda_n) \sim 0.2$ .

Comparing Figs. 7 and 4, one can conclude that two different numerical methods lead to very similar results. The numerical data of the both methods are also in a good agreement with the trajectory results shown by the dots in Figs. 4 and 7.

## VII. DISCUSSIONS

A common point of view is that due to intrinsic underbarrier mechanisms a magnetic field always reduces a probability of tunneling decay of a metastable state. In other words, it never chances to get tunneling rate enhanced by a magnetic field for many orders of magnitude. This point of view is supported by a general arguments that in the classical electrodynamics a motion ahead is prevented by cyclotron rotation and the same happens in quantum mechanics. The famous example is Landau states. The increased localization of a wave function in a magnetic field can also be explained by an additional potential, proportional to squared velocity, created by the magnetic field. Any hand waving explanation leads to a conclusion of tunneling reduction. We propose a mechanism which contrasts to that point of view.

Cyclotron enhancement of tunneling is clear for understanding. It occurs due to a rotation under the barrier of a velocity vector of the electron. Under the cyclotron rotation it becomes more aligned with the tunneling direction, which increases the tunneling rate. A necessary condition for the phenomenon is a finite velocity (17) in the decayed state of the quantum wire. The velocity should be directed along the vector  $\vec{\mathcal{E}}_0 \times \vec{H}$ , which is parallel to the wire. In the case of the opposite direction the magnetic field reduces the tunneling rate. For cyclotron enhancement of tunneling it is important that a sample, from where tunneling occurs, should be extended in the direction perpendicular to tunneling. The effect is absent in tunneling from a small quantum dot.

The scenario of decay of the metastable state in the magnetic field consists of two parts. First, the electron moves under the barrier rotating its velocity. On this step, a role of reflections from the restricting walls is minor. Second, after exit from under the barrier the electron goes to infinity performing multiple reflections from the restricting walls.

The semiclassical approach used is confirmed by two different numerical methods. A domain of parameters for the phenomenon can be roughly estimated from the

condition that the Lorentz force, caused by the velocity in the wire, is of the order of the potential force  $\mathcal{E}_0$ . The parameter  $h$  is

$$h = B \frac{\hbar\omega_c}{2u_0} \simeq 0.58 \times 10^{-4} B \frac{H(\text{Tesla})}{u_0(\text{eV})}. \quad (45)$$

Since we are interested in  $h \sim 1$  and the semiclassical parameter  $B$  is large, the Landau splitting  $\hbar\omega_c$  is always less than  $u_0$  which defines a scale of the energy levels in the quantum wire.

To be specific, let us consider different regimes of tunneling.

*Strong effect on tunneling ( $h = 2$ ).* We take  $B = 40$  and  $\lambda = -0.3$ . Then at zero magnetic field the tunneling rate (22) is  $6.9 \times 10^{-24}$ . At  $h = 2.0$  the tunneling rate (22) becomes  $1.1 \times 10^{-7}$ . The enhancement occurs under the condition  $u_0(\text{eV}) \simeq 1.16 \times 10^{-3} H(\text{Tesla})$ . For reasonable values of the magnetic field,  $H \simeq 10$  Tesla, the quantum wire or the thin film should be “soft” in the sense of a not large  $u_0 \sim 0.01$  eV. See Refs. [15, 16, 23]. The exit point from under the barrier is estimated as  $x_0 \simeq 250 \text{ \AA}$  and the electric field is  $\mathcal{E}_0 \simeq 1.3 \times 10^3$  eV/cm.

*Weak effect on tunneling ( $h = 0.2$ ).* We take  $B = 15.8$  and  $\lambda = -0.3$ . Then at zero magnetic field the tunneling rate (22) is  $7.1 \times 10^{-10}$ . At  $h = 0.2$  the tunneling rate (22) becomes  $1.0 \times 10^{-7}$ . The enhancement occurs under the condition  $u_0(\text{eV}) \simeq 1.16 \times 10^{-2} H(\text{Tesla})$ . For reasonable values of the magnetic field,  $H \simeq 10$  Tesla, one can choose  $u_0 \sim 0.1$  eV. The exit point from under the barrier is estimated as  $x_0 \simeq 75 \text{ \AA}$  and the electric field is  $\mathcal{E}_0 \simeq 1.0 \times 10^5$  eV/cm.

One can conclude that an experimental observation of cyclotron enhancement of tunneling is possible. An experimental arrangement can be a quantum wire embedded into a two-dimensional electron system. The electric field is parallel to the two dimensional system and is perpendicular to the wire. The magnetic field is perpendicular to the wire and to the electric field. One can use a dielectric wall parallel to the tunneling direction just to get electrons moved away after tunneling along the wall due to multiple reflections from it in the magnetic field.

Another way of an experimental observation is to use a thin film, with a quantized motion inside, perpendicular to the electric field.

## VIII. CONCLUSIONS

A magnetic field can enhance a tunneling decay rate of a metastable state for many orders of magnitude. This happens due to intrinsic underbarrier mechanisms of a cyclotron rotation of an electron velocity. It becomes more aligned with the tunneling direction resulting in the enhancement of the tunneling rate. The effect can be observed experimentally for tunneling from a quantum wire or a thin film across a barrier created by an applied electric field.



### Acknowledgments

We thank S. V. Iordanski for valuable discussions. This work was partially supported by Russian Foundation for

Basic Research and “Financiadora de Estudos e Projetos - FINEP” and Brazilian “Ministério da Ciência e Tecnologia - MCT”.

- 
- [1] B. I. Shklovskii, Pis'ma Zh. Eksp. Teor. Fiz. **36**, 43 (1982) [Sov. Phys. JETP Lett. **36**, 51 (1982)].
- [2] B. I. Shklovskii and A. Efros, Zh. Eksp. Teor. Fiz. **84**, 811 (1983) [Sov. Phys. JETP **57**, 470 (1983)].
- [3] Q. Li and D. Thouless, Phys. Rev. B **40**, 9738 (1989).
- [4] G. Blatter and V. Geshkenbein, in *The Physics of Superconductors*, edited by K.H. Bennemann and J.B. Ketterson (Springer-Verlag Berlin Heidelberg New York, 2003).
- [5] D. A. Gorokhov and G. Blatter, Phys. Rev. B **57**, 3586 (1998).
- [6] A. V. Khaetskii and B. I. Shklovskii, Zh. Eksp. Teor. Fiz. **85**, 721 (1983) [Sov. Phys. JETP **58**, 421 (1983)].
- [7] J. Hajdu, M. E. Raikh, and T. V. Shahbazyan, Phys. Rev. B **50**, 17625 (1994).
- [8] H. A. Fertig and B. I. Halperin, Phys. Rev. B **36**, 7969 (1987).
- [9] T. Sharpee, M. I. Dykman, and P. M. Platzman, Phys. Rev. B **65**, 032122 (2002).
- [10] B. Ivlev, Phys. Rev. A **73**, 052106 (2006).
- [11] B. Ivlev, Phys. Rev. A **76**, 022108 (2007).
- [12] L. D. Landau and E. M. Lifshitz, *Quantum Mechanics* (Pergamon, New York, 1977).
- [13] W. Demmerle, J. Smoliner, E. Gornik, G. Böhm, and G. Weimann, Phys. Rev. B **47**, 13574 (1993).
- [14] P. H. Beton, J. Wang, N. Mori, L. Eaves, P. C. Main, T. J. Foster, and M. Henini, Phys. Rev. Lett. **75**, 1996 (1995).
- [15] E. E. Vdovin, Yu. N. Khanin, O. N. Makarovskiy, Yu. V. Dubrovskii, A. Patane, L. Eaves, M. Henini, C. J. Mellor, K. A. Benedict, and R. Airey, Phys. Rev. B **75**, 115315 (2007).
- [16] E. E. Vdovin, A. Levin, A. Patane, L. Eaves, P. C. Main, Yu. N. Khanin, Yu. V. Dubrovskii, M. Henini, and G. Hill, Science **290**, 122 (2000).
- [17] L. D. Landau and E. M. Lifshitz, *The Classical Theory of Fields* (Butterworth-Heinemann, Oxford, 1998).
- [18] C. G. Callan and S. Coleman, Phys. Rev. D **16**, 1762 (1977).
- [19] S. Coleman, in *Aspects of Symmetry* (Cambridge University Press, Cambridge, 1985).
- [20] A. Schmid, Ann. Phys. **170**, 333 (1986).
- [21] U. Eckern and A. Schmid, in *Quantum Tunneling in Condensed Media*, edited by A. Leggett and Yu. Kagan (North-Holland, Amsterdam, 1992).
- [22] J. P. Palomarez-Baez, B. Ivlev, and J. L. Rodriguez-Lopez, Phys. Rev. A **76**, 052103 (2007).
- [23] W. G. van der Wiel, S. De Franceschi, J. M. Elzerman, T. Fujisava, S. Tarucha, L. P. Kouwenhoven, Rev. Mod. Phys. **75**, 1 (2003).